Structural Differences between *Saccharomyces cerevisiae* Ribosomal Stalk Proteins P1 and P2 Support Their Functional Diversity†

J. Zurdo,‡,§ Carlos González,|| Jesús M. Sanz,⊥ Manuel Rico,|| M. Remacha,‡ and J. P. G. Ballesta*,‡

Centro de Biología Molecular "Severo Ochoa" (CSIC and UAM), Canto Blanco, 28049 Madrid, Spain, Instituto de Estructura de la Materia, (CSIC), Serrano 117, 28006 Madrid, Spain, and Centro de Biología Molecular y Celular, Universidad Miguel Hernández, Elche, 03206 Alicante, Spain

Received February 15, 2000; Revised Manuscript Received April 19, 2000

ABSTRACT: The eukaryotic acidic P1 and P2 proteins modulate the activity of the ribosomal stalk but playing distinct roles. The aim of this work was to analyze the structural features that are behind their different function. A structural characterization of *Saccharomyces cerevisaie* P1α and P2*β* proteins was performed by circular dichroism, nuclear magnetic resonance, fluorescence spectroscopy, thermal denaturation, and protease sensitivity. The results confirm the low structure present in both proteins but reveal clear differences between them. P1α shows a virtually unordered secondary structure with a residual helical content that disappears below 30 °C and a clear tendency to acquire secondary structure at low pH and in the presence of trifluoroethanol. In agreement with this higher disorder P1α has a fully solvent-accessible tryptophan residue and, in contrast to P2*β*, is highly sensitive to protease degradation. An interaction between both proteins was observed, which induces an increase in the global secondary structure content of both proteins. Moreover, mixing of both proteins causes a shift of the P1α tryptophan 40 signal, pointing to an involvement of this region in the interaction. This evidence directly proves an interaction between P1α and P2*β* before ribosome binding and suggests a functional complementation between them. On a whole, the results provide structural support for the different functional roles played by the proteins of the two groups showing, at the same time, that relatively small structural differences between the two stalk acidic protein types can result in significant functional changes.

The ribosome is formed by a number of structural domains, which can probably be assembled autonomously (*1*), and in some cases have a very specific function in the translation process. One the best characterized and functionally relevant domains is the ribosomal stalk, a very flexible lateral protuberance of the large ribosomal subunit of bacteria (*2*). In *Escherichia coli*, the stalk was found to be formed by two dimers of the acidic proteins L7/L12 (*3*), which form a highly stable complex with one molecule of protein L10 (*4*, *5*). This pentamer binds to the highly conserved GTPase-related center in the 23S rRNA (*6*, *7*). The stalk, on the other hand, has been biochemically shown to play an important role in the function of the elongation factors during protein synthesis (*8*), as was recently confirmed by cryo-electron-microscopy (*9*, *10*)

A similar structure to the bacterial stalk is present in the ribosome from all organisms (*11*). Moreover, proteins equivalent to the bacterial L7/L12 and L10 have also been found in all the species analyzed, including eukaryots (*12*), archea (*13*, *14*), and organelles (*15*). As in bacteria, the basic functional role of the stalk in other organisms seems to be related to the elongation factor activities (*16*−*18*). However, the eukaryotic stalk displays a set of properties that suggest it may have regulatory functions nor found in other systems (*12*).

Not surprisingly, the eukaryotic stalk is more complex than the bacterial one. A single bacterial acidic protein (L7 corresponds to the N-terminal blocked form of L12) has evolved to a family of proteins formed by at least two members which were given different names, but are now generally called P1 and P2 (*19*) due to the fact that they are found phosphorylated in the ribosome (*20*−*23*). In some species more than one protein of each type is present (*12*), and the presence of even a third acidic protein type, called P3, was recently reported in plants (*24*). In *Saccharomyces cerevisiae*, two forms of P1 and P2, P1α/P1*β* and P2α/P2*β*, are present (*25*). The eukaryotic P1 and P2 proteins form a complex with protein P0 and the 28S rRNA GTPase domain which can be isolated after degradation of the ribosome with RNAse (*26*). The stability of this structure is, however, considerably lower than in bacteria, since contrary to L7/L12, the P1/P2 proteins in the complex can exchange with those present in a cytoplasmic pool of these proteins (*20*, *27*, *28*). In contrast, protein P0 binds more tightly to the rRNA and is not removed in conditions under which L10 protein is easily extracted from the bacterial ribosome (*29*).

† This work was supported by Grant PB94-0032 from the Dirección General de Política Científica and by an institutional grant to the Centro de Biología Molecular from the Fundación Ramón Areces.

* To whom correspondence should be addressed. Phone: +34-91-3975076. Fax: +34-91-3974799. E-mail: jpgballesta@cbm.uam.es.

‡ Centro de Biología Molecular "Severo Ochoa".

§ Present address: Oxford Centre for Molecular Sciences, New Chemistry Laboratory, Oxford OX1 3QT, U.K.

|| Instituto de Estructura de la Materia.

⊥ Centro de Biología Molecular y Celular.

10.1021/bi000363b CCC: $19.00 © 2000 American Chemical Society
Published on Web 07/06/2000

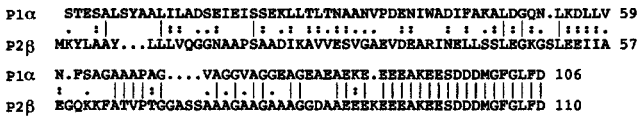

FIGURE 1: Sequence comparison between yeast P1α and P2*β*. Alignments were carried out using the program FASTA.

Contrary to the functional irrelevancy of the presence of two forms of acidic proteins in bacteria (*30*), the different eukaryotic acidic ribosomal proteins do not have the same function (*31*). The different members of the P1 and P2 families are encoded by independent genes, and although they have a notable overall amino acid sequence similarity, they also show substantial structural differences, especially at the amino terminal domain (*12*) (Figure 1), which is the part of the protein involved in the interaction with the ribosome (*32*).

Previous results have pointed out that inactivation of the *S. cerevisiae* genes encoding both members of the same type, either P1 or P2, resulted in the absence of any acidic protein in the ribosome (*33*). These results seemed to indicate that the presence of both protein types was required for the formation of the stalk protein complex with protein P0. It has been recently found, however, that the P2 proteins accumulate free in the cells when the P1 protein gene is deleted while the P1 proteins are degraded in the absence of P2 (G. Nusspaumer, M. Remacha, and J. P. G.Ballesta, unpublished results). These data indicate that while P2 proteins do seem indeed to require the presence of P1 for ribosome binding, the reverse is not fully established. In fact, it has been found that P1 proteins are able to bind to the ribosome in the absence of P2 but not the other way around (*34*), underscoring the important structural differences that exist between these two protein types.

In a previous report, the structure of the acidic protein P2*β*, one of the two forms of the P2 group in *S. cerevisiae*, was studied using different approaches. The results indicated important structural differences with respect to the bacterial proteins. Contrary to L7/L12, which has a well structured C-terminal domain (*35*), the eukaryotic protein lacks a stable tertiary structure when free in solution, and it has a rather loose structure that looks like a molten globule conformation (*36*).

To further explore the structural relationship between the different acidic protein families and to understand their clearly different functional roles a study of yeast protein P1α has been performed. A structural characterization of P1α as well as its comparison with P2*β* has been carried out using different biophysical methods. The results show clear structural differences between the two proteins and provide evidence for their interaction, which promotes an increase in the global secondary structure of the complex.

EXPERIMENTAL PROCEDURES

Expression and Purification of the Protein. The recombinant yeast ribosomal acidic protein P2*β* was purified as previously described (*36*) except that the cell lysate was directly loaded onto a DEAE-Sepharose column, and after elution using a 0 to 500 mM NaCl linear gradient in 20 mM Tris-HCl, pH 7.8, protein was concentrated and loaded onto a Sephacryl S100 column. Recombinant P1α was purified in a similar way from *E. coli* BL21(DE3)plac previously transformed with a pT7-7 vector (*37*) carrying the P1α gene. Cells were grown at 37 °C in TB medium (200 mg/L ampicillin) up to A600 = 2.0, and then induced with 0.4 mM IPTG. Protein induction as well as cell harvesting and disruption was done as previously described (*36*). The clear lysate was adsorbed on DEAE-Sepharose, and protein was then eluted using a 0 to 500 mM NaCl linear gradient in 20 mM Tris-HCl, pH 7.8. The protein, which eluted as one peak at around 230 mM NaCl, was concentrated by Macrosep 3 kDa exclusion limit ultrafiltration tubes, loaded onto a preequilibrated Sephacryl S100 column and eluted with 50 mM NaCl and 20 mM Tris-HCl, pH 7.8. The P1α protein peak was again loaded onto a DEAE-Sepharose column, and eluted employing the same gradient previously described. The protein was finally dialyzed against water, lyophilized, and stored at −20 °C. When necessary, buffer exchange and concentration of protein were carried out in ultrafiltration tubes.

Protein Analysis. Electrophoresis and isoelectrofocusing were performed as described before (*38*). Electrospray mass spectrometry measurements were made by the Peptide and Nucleotide Laboratory, Dept. of Organic Chemistry, Universidad de Barcelona. Protein sequencing was performed on an Applied Biosystems 473A protein sequencer in the Protein Chemistry Service (Centro de Biología Molecular "Severo Ochoa"). Western blot and ELISA assays were carried out using both a set of specific monoclonal antibodies to P1α, P2*β*, and the C-terminal domain of all the P proteins (*39*). Also a polyclonal antiserum raised against a truncated P1α protein lacking the conserved C-terminal domain (C. Santos and J. P. G. Ballesta, unpublished results) was used.

Identity of the Recombinant Proteins. P1α was identified by automatic Edman degradation. The resulting sequence S-T-E-S-A corresponds to the N-terminal of the corresponding gene-encoded protein (*40*) but without the initiating methionine. Contrary to the native protein (*41*), the recombinant P1α was found not N-acetylated. Moreover, electrospray mass spectrometry results of the protein was in accordance with the expected molecular mass of the unblocked polypeptide. In all the cases both the polyclonal antiserum against native P1α, as well as monoclonal antibodies against the C-terminal region of the P proteins cross-reacted with the purified polypeptide (data not shown). The identity of protein P2*β* was confirmed using similar approaches as previously reported (*36*).

Protein Estimation. Protein concentrations were determined from the absorbance at 280 nm using an extinction coefficient of 6970 M^{-1} cm^{-1} in water, calculated from the amino acid composition of the protein (*42*).

Circular Dichroism. Circular dichroism (CD)[1] spectra were collected on a Jasco J720 spectropolarimeter fitted with a thermostated cell holder and interfaced with a Neslab RTE-110 water bath. Isothermal wavelength spectra were acquired at 25 °C. Protein was initially dissolved in 20 mM potassium phosphate, pH 7.0, and the pH adjusted as required by adding either H_3PO_4 or NaOH. Additionally, 20 mM glycine, pH 2.0, was used as a buffer in some CD experiments. Far-UV

[1] Abbreviations: CD, circular dichroism; NMR, nuclear magnetic resonance; IPTG, isopropyl-*β*-D-thiogalactopyranoside; TFE, 2,2,2-trifluoroethanol; [Θ], molar ellipticity; SDS−PAGE, sodium dodecylsulphate polyacrylamide gel electrophoresis.

CD measurements were done using 40−60 μg/mL of protein in either a 1 or 2 mm path cuvette. Near-UV CD spectra were obtained on a 1−2 mg/mL protein solution in a 10 mm path cuvette. Ellipticities ([Θ]) are expressed in units of degrees squared centimeters per decimole, using the mean residue concentration of the protein. Thermal denaturation experiments were performed using a heating rate of 20 °C h^{-1} and a response time of 2 s. Thermal scans were collected from 5 to 85 °C in 2 mm cells at a protein concentration of 40−60 μg/mL. Reversibility of the thermal transitions was checked by recording a new scan after cooling the thermally denatured sample and comparing it with the spectra obtained before heat denaturation.

Secondary Structure Prediction and Circular Dichroism Analysis. Secondary structure content of both P1α and P2β was predicted using PHD (*43*−*45*). Estimation of the amount and type of secondary structure of both proteins from their far-UV spectra was carried out using different deconvolution methods: CDNN (*46*), K2D (*47*), and some of the fitting routines included in the Dicroprot software (*48*) such as least-squares fitting methods (*49*, *50*), SELCON (self-consistent method) (*51*) and VARSELECT (Variable Selection method) (*52*, *53*). The approximate α-helical content of the proteins was estimated from their molar ellipticity at 220 nm ($[\Theta]_{220}$) according to ref *50*.

Fluorescence Spectroscopy. Fluorescence experiments were performed on a Perkin-Elmer LS-B spectrofluorimeter. Protein concentration was 60 μg/mL and buffers were the same as in CD measurements. Tryptophane intrinsic fluorescence spectra were recorded from 310 to 510 nm at a scan speed of 100 nm/min (slit 8 nm) upon excitation at 295 nm (slit 2 nm). Blanks without protein were subtracted from the spectra. Quenching experiments were carried out using acrylamide previously equilibrated in the desired buffer. Protein concentration was typically 60 μg/mL whereas acrylamide concentration varied from over 0 to 500 mM. Quenching of the intrinsic Trp40 fluorescence of P1α by acrylamide was analyzed according to refs *54* and *55*. P1α and P2β interaction experiments were carried out monitoring P1α Trp40 emission using a constant concentration of P1α and adding increasing amounts of P2β. Fluorescence results were analyzed according to ref *56* to obtain a binding constant. Only P2β concentrations up to 5 μM were used for calculation purposes.

Nuclear Magnetic Resonance Spectroscopy. ^{1}H NMR experiments were carried out on a Bruker 600 MHz spectometer. One-dimensional spectra were recorded at 25 °C (unless another temperature is indicated) with 16K data points and using presaturation to eliminate the water signal. Data were processed with the Bruker software UXNMR. Sample concentration was typically 1−2 mg/mL. D_2O experiments were carried out with freshly prepared samples from protein aliquots freeze-dried in H_2O.

Proteolysis Assays. Proteinase resistance was evaluated after incubating protein samples with Proteinase K (proteinase concentration was 10 μg/mL in 20 mM potassium phosphate, pH 7.0, and different concentrations of TFE) at 30 °C for 2 h. Samples were later loaded onto a 10−15% discontinuous SDS−PAGE gel (*57*) to resolve undigested fragments. Identification of the resistant fragments was made using both N-terminal sequencing and electrospray mass spectrometry as described above.

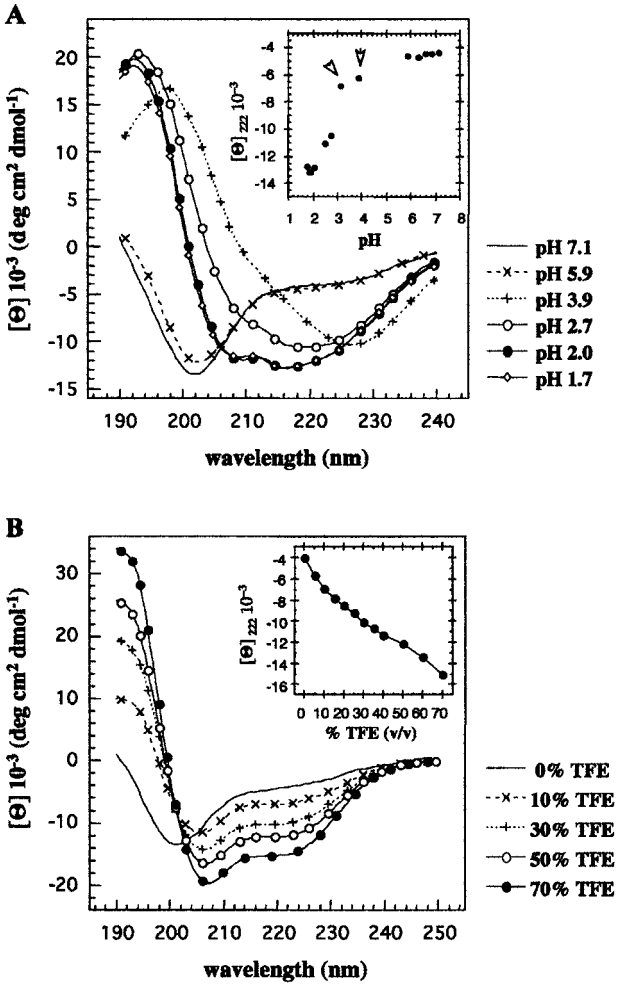

FIGURE 2: Far-UV CD analysis of protein P1α. (A) Effect of different pH values on the secondary structure content of yeast P1α. (Insert) Ellipticity at 222 nm as a function of pH. Arrows indicate some turbidity in the sample, probably because of pH proximity to the pI of the protein. (B) TFE titration of P1α monitored by far-UV CD. (Insert) Ellipticity at 222 nm as a function of TFE content.

Chemical Cross-Linking. P1α self-association was tested by cross-linking as reported previously (*36*). P1α samples (0.5 and 1.0 mg/mL) in 20 mM phosphate buffer, pH 7.0, were incubated in the presence of 5 mM glutaraldehyde for 10 min at 25 °C. The reaction was stopped by adding 3 vol of acetone:acetic acid (9:1) to the samples and keeping them at −20 °C for 1 h. The precipitated protein was collected by centrifugation at 13 000 rpm for 15 min, dried by vacuum, and resuspended in a loading buffer. Different species were resolved by SDS−PAGE using precasted NuPAGE(TM) 10% Bis-Tris gels (Novex, Invitrogen).

RESULTS

Structural Characterization of P1α. Far-UV CD measurements were carried out to characterize the secondary structure content of P1α in solution (Figure 2). The P1α CD spectra show features of a virtually unordered protein with some negative ellipticiy around 222 nm which disappears completely when high concentrations of urea are added to the protein (data not shown). This suggests a residual α-helical content even though the protein seems to be mainly random-coil. Surprisingly, the far-UV CD spectrum changes dramatically when the pH decreases and an increase in the secondary

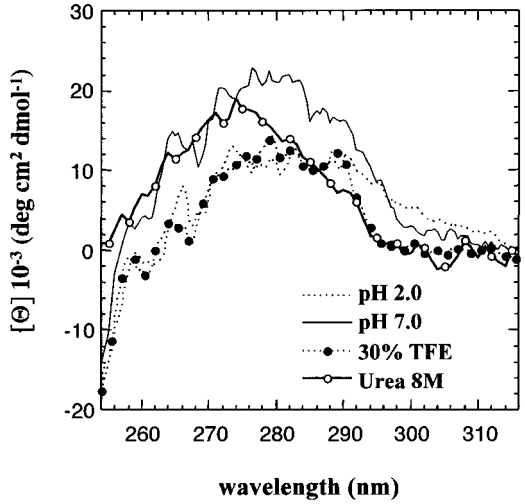

FIGURE 3: Near-UV CD spectra of P1α. Spectra were collected in either 20 mM potassium phosphate, pH 7.0; or 20 mM glycine, pH 2.0. Urea 8 M, and 30% TFE were added as indicated.

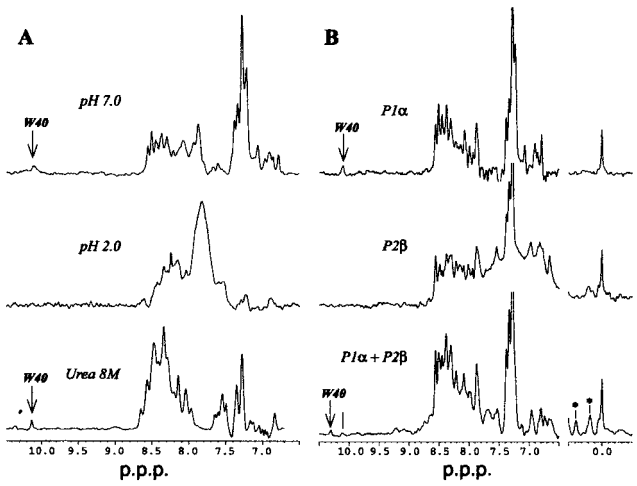

FIGURE 4: 1D-NMR spectra of P1α and effect of P2β. Experiments were carried out with the protein under the same conditions indicated in Figure 3. W40 indicates the position of the aromatic NH proton of tryptophan 40. In panel B, an equimolecular mixture of P2β and P1α (total protein concentration 0.1 mM) in 20 mM potasium phosphate, pH 7.0, was used to evaluate the possible interaction between both proteins and their structural effects. The position of P1α Trp40 signal is indicated as W40. New signals that arose in the aliphatic region after the interaction are also indicated (*).

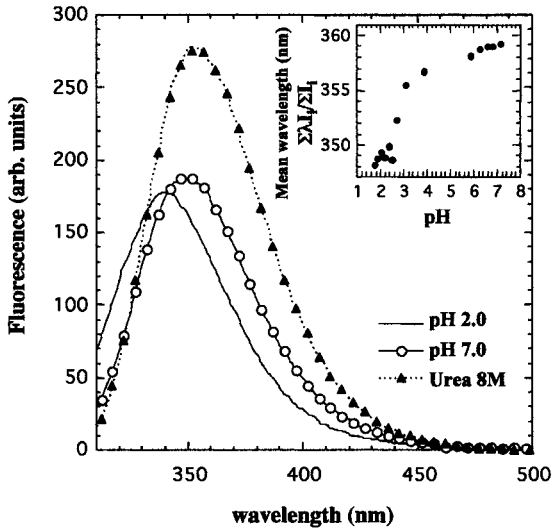

FIGURE 5: Intrinsic fluorescence of P1α. Effect of pH and urea denaturation. Trp40 emission spectra were collected at pH 7.0 and 2.0 (see Figure 3) and in the presence of urea 8 M. (Insert) pH titration. Changes in Trp40 wavelength emission were monitored using the "mean wavelength" ($\Sigma\lambda I/\Sigma I$, where λ is wavelength and I is the intensity at a given wavelength) to better detect shifts in the fluorescence signal.

structure content of the polypeptide appears (Figure.2A). TFE addition also has a pronounced effect on the far-UV P1α CD spectrum, bringing about an almost linear increase in the α-helix content of the protein (Figure.2B). The linearity of the response supports the unordered structure of the protein at physiological pH values, since no cooperative transition is observed as could be expected from a compact polypeptide. Therefore, a mainly random-coil conformation can be attributed to the protein, and the contribution of β features can be discarded. Nevertheless, this might not be the case at pH values where the protein aggregates (close to its pI) or at pH close to 2.0 (see NMR results below). Both pH and TFE titrations were carried out at different concentrations in the admissible range for far-UV CD without important alterations (data not shown).

Near-UV CD spectra of P1α at a neutral pH show a maximum centered at 280 nm (Figure 3), probably indicating that the tryptophan 40 and/or the tyrosine 8 show optical activity, probably due to their placement in some asymmetrical or constrained environment. This signal does not disappear but decreases slightly either at pH 2.0 or after incubation in TFE. Moreover, the signal remains mainly unaffected at 8 M urea, albeit the whole secondary structure content of the protein is lost under these conditions. Therefore, the near-UV CD signal exhibited by P1α seems to be unrelated to any long distance interaction, tertiary fold feature or the presence of any hydrophobic/aromatic core. On the contrary, this signal is more likely to be due to some kind of local interaction (i.e., neighboring hydrophobic residue) that alters the symmetry of the aromatic residues, and promotes optical activity in this spectral region.

Nuclear Magnetic Resonance. In agreement with the previous observations, NMR studies on the intact protein show very little signal dispersion (Figure 4) and very fast amide exchange when protein is incubated in the presence of deuterated water (data not shown). Nevertheless, a detailed exchange analysis was not feasible, since both aggregation and secondary structure changes occur at low pH values, and no "stable" form to quench the amide exchange is known for the protein. NMR spectra from urea denatured protein show no dramatic differences from the native one in terms of signal dispersion, confirming the unfolded character of the protein. These small differences could arise from some residual secondary structure still present in the protein (see above). Signal broadening can also be observed at a low pH as a possible indication of protein aggregation. Therefore, stabilization of the secondary structure of the protein upon oligomerization at low a pH cannot be ruled out.

Intrinsic Fluorescence and Quenching Experiments. The intrinsic fluorescence spectrum of the tryptophan 40 (Trp40) in P1α shows a maximum centered at 346 nm, which shifts to the blue at acidic pH values (Figure 5). This feature could be due to the "hiding" of this residue inside the protein or by formation of aggregates. The enhancement of fluorescence when high concentrations of urea are added suggests the

Table 1: P1α Tryptophane Quenching by Acrylamide

sample	K (M^{-1})	V (M^{-1})	K_{sv}^{eff} (M^{-1})[a]
pH 7.0	9.39	1.59	12.91
pH 2.0	2.35	0.90	3.85
urea 8 M	8.12	2.02	11.65

[a] In all the cases f_a^{eff} was >1.

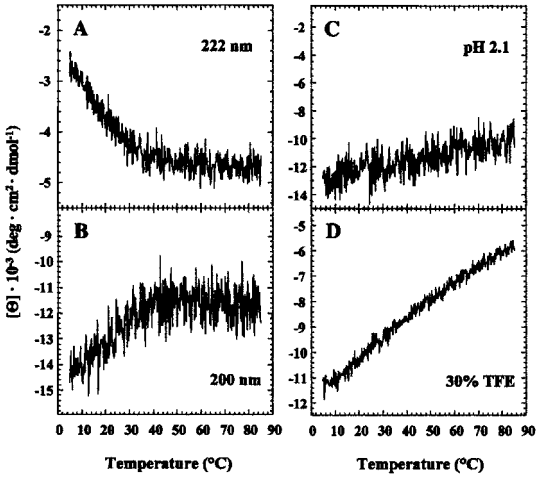

FIGURE 6: Thermal denaturation of P1α. Thermal denaturation patterns exhibited by P1α at pH 7.0 monitored at 200 (A) and 222 nm (B); and at pH 2.1 (C) and 30% TFE (D), both monitored at 222 nm.

existence of an intrinsic quencher next to the Trp residue, which could be partially responsible for the near-UV CD signal shown by the protein.

To explore the degree of solvent exposure of Trp40 under different conditions quenching experiments with acrylamide were carried out (Table 1). From these data it can be concluded that the exposure degree shown by the Trp40 at pH 7.0 is similar to the one exhibited at high urea concentrations, and therefore indicates the absence of a hidden aromatic core in the protein. The low quenching constants determined for the protein at pH 2.0 support the protection of the Trp residue at those pH values. As the shift in the wavelength of the emission suggested (see above), this effect could be caused either by the constraint of the Trp surroundings or by Trp hiding due to protein aggregation. It is interesting to notice that maximum degree of shifting follows a pattern similar to the one shown by the changes in the secondary structural content of the protein (inset Figure 5, see also Figure 3A).

Thermal Denaturation. Thermal denaturation of P1α monitored by UV−CD was carried out under different conditions to further characterize the structure of the protein. P1α seems to show a slightly cooperative cold denaturation at a neutral pH, since there is an increase in ellipticity at 200 nm together with a decrease at 222 below 30 °C (Figure 6, panels A and B). These results support the existence of some residual helical content under physiological temperatures, which could be important for P1α function. It is interesting to note that the denaturation profiles at pH 2.0 and in the presence of 30% TFE are linear (Figure 6, panels C and D), supporting the absence of specific tertiary contacts at any temperature, even though a secondary structure appears in these conditions. Moreover, the very small changes in ellipticity observed at pH 2.1 could be due to an additional stabilization of the protein upon aggregation as suggested previously.

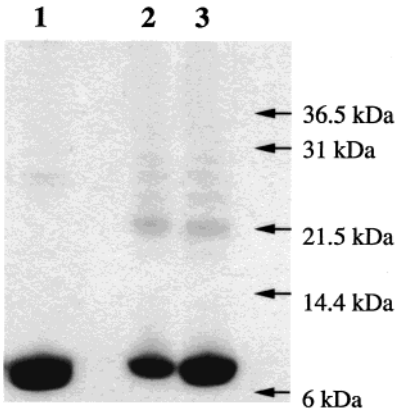

FIGURE 7: P1α self-association. SDS−PAGE of P1α after chemical cross-linking in the presence of glutaraldehyde (lanes 2 and 3) as described in Experimental Procedures. Protein in the absence of cross-linker is included as a reference (lane 1). Two different concentrations of P1α, 0.5 mg/mL (lane 2) and 1.0 mg/mL (lane 3), were tested. The position of the molecular weight markers is indicated.

Table 2: P1α and P2β Secondary Structure Content Estimated from Far-UV CD Measurements[a]

	P1α			P2β		
	helix	extended	other	helix	extended	other
ellipticity 220 nm	0.11			0.24		
Chen[c]	0.10	0.05	0.87	0.25	0.13	0.62
Bolotina	0.10	0.09	0.83	0.24	0.11	0.65
SELCON	nd	nd	nd	0.31	0.08	0.61
VARSLC	nd	nd	nd	0.34	0.14	0.52
K2D	0.08	0.42	0.50	0.26	0.15	0.59
CDNN	0.16	0.28	0.56	0.31	0.22	0.48
PDH[b]	0.68	0.00	0.32	0.66	0.00	0.34

[a] Total secondary structure is adjusted for 1.00. Only estimations in the interval of 1.00 ± 0.10 and RMSD < 0.25 were considered. RMSD > 0.25 or sum of secondary structure values > 1.00 ± 0.10 appear as nd. [b] PDH is a prediction based on the protein sequence, not on the CD data. [c] Spectra analysis was carried out as indicated in Experimental procedures.

P1α Self-Association. Chemical cross-linking has been used to test the capacity of P1α to self-associate under physiological conditions (Figure 7). At a 0.5−1.0 mg/mL concentration, the monomeric protein is almost the only one observed, with traces of aggregated species that could correspond to protein dimers. Similar experiments carried out on P2β showed a high proportion of dimers and tetramers under comparable concentrations (*36*). It seems, therefore, that P1α shows a much lower self-association propensity than does P2β.

Structural Differences between P1α and P2β. An analysis of the P1α and P2β sequences with the PHD program predicts a high content in α-helix (Table 2) concentrated mainly in the N-terminal region of both polypeptides. The predicted secondary structure pattern is quite similar for both proteins (Figure 8) and suggests the existence of a "structured" region of the protein expanding the main part of the sequence followed by a less defined one (rich in "loops"). The predicted topology agrees with the location of the "hinge" region in P2β, established by sequence identity comparisons with its prokaryotic counterpart L7/L12 (*36*).

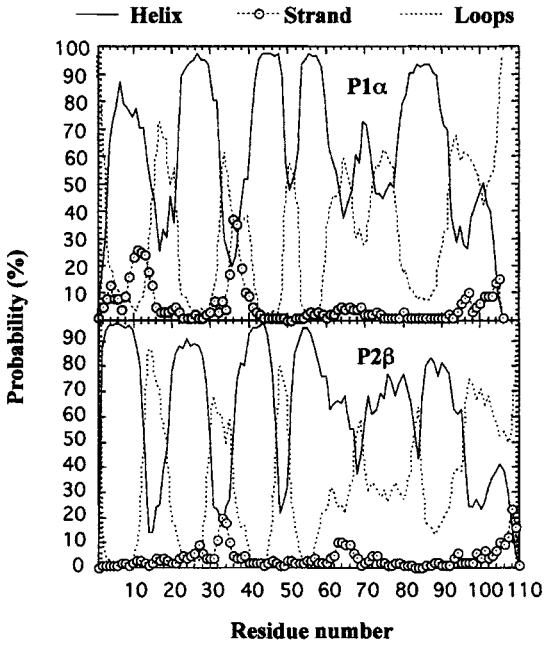

FIGURE 8: Secondary structure prediction for P1α and P2*β*. Prediction was performed using PDH software (see Experimental procedures).

Despite this apparent similarity, the comparison of experimental data for P1α in this report and those for P2*β* previously reported (*36*) indicate clear structural differences between P1α and P2*β* that support their nonidentical function. In this way, the far-UV spectra of both proteins show considerable differences (Figure 9A). Thus, whereas P2*β* shows a clear helical pattern, P1α resembles a random coil. Moreover, deconvolution analysis of both spectra by different methods indicates an average helical content of around 28% for P2*β*, whereas it is only 11% for P1α. It is interesting to note, however, that these values are far from the one estimated by PDH (Table 2).

It must be also mentioned that some secondary structure analysis programs indicate some *β*-sheet structure content although the spectroscopic data do not agree with the presence of this structural element in the monomeric proteins. It is well-known that whereas estimation of α-helical content from CD data is well established, other structural elements are more difficult to identify due either to their structurally less defined state or to the overlap of their CD spectral components (*58*). However, the possibility that this *β* contribution might be associated to interchain contacts in the oligomers (mainly dimers) that are present at the protein concentrations used for CD analysis (*36*) cannot be ruled out.

The different sensitivity to proteolysis also reveals the differences between both proteins. Proteinase K digestion of both P1α and P2*β* was carried out in the absence and in the presence of increasing amounts of TFE to stabilize the secondary structure of the proteins. Electrophoresis of the products obtained (Figure 10), clearly shows the protection of a P2*β* protein fragment even at low TFE concentrations, whereas P1α is completely degraded in all conditions tested. Characterization of the P2*β* proteinase K-resistant fragment by N-terminal sequencing and electrospray mass spectrometry indicated the presence of a mixture of two peptides that

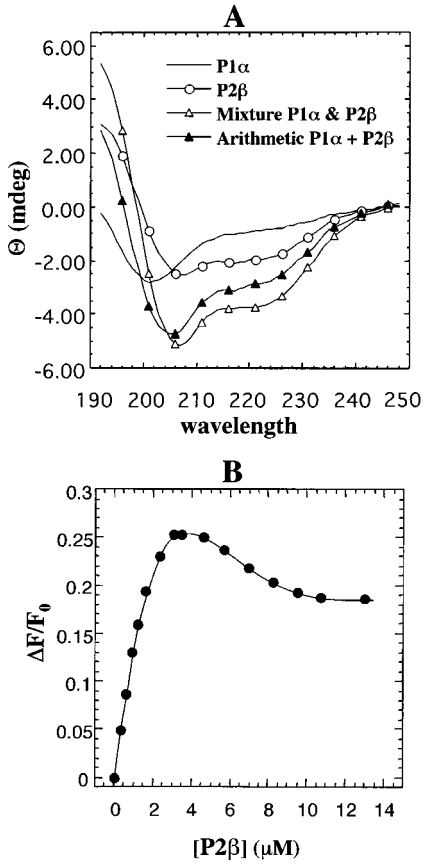

FIGURE 9: Effect of P1α−P2*β* interaction. (A) Far-UV CD of an equimolecular mixture of P1α and P2*β* in 20 mM potassium phosphate, pH 7.0, and comparison with the arithmetic addition of spectra of both proteins in the same buffer and concentration conditions (protein concentration was 6 *μ*M). (B) Enhancement of the P1α Trp40 fluorescence emission upon addition of P2*β*. Artifacts due to protein aggregation and fluorescence quenching can be observed at higher P2*β* concentrations.

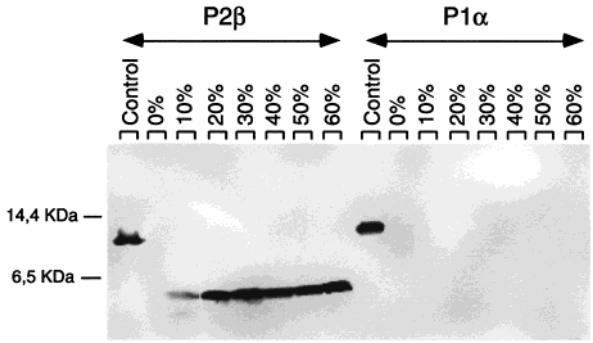

FIGURE 10: Proteinase K sensitivity of P1α and P2*β*. Proteins were dissolved in 20 mM potassium phosphate, pH 7.0, in the presence of different amounts of TFE and resolved by SDS−PAGE (see Experimental procedures). The "Control" lanes contain the proteins in the absence of proteinase, and the rest of the lanes contain samples subjected to digestion at different TFE rates. Proteinase concentration was 10 *μ*g/mL. The position of molecular weight markers is indicated.

expand the first 70 and 72 residues respectively, including the amino terminal end of the protein (Figure 1).

P1α/P2β Protein Interaction. Since there are data suggesting an interaction of protein P1α and P2*β* inside the cell, a direct confirmation of this possibility was sought in vitro. Incubation of both proteins was followed by far-UV CD and 1D-NMR measurements, and spectra were compared with

those of the isolated proteins under the same conditions. The CD spectra of the protein mixture, when compared to the arithmetical addition of spectra from the individual proteins indicate that some secondary structural changes take place upon incubation of both proteins together (Figure 9A). Protein interaction seems to increase the secondary structural content (α-helical content) of one or both proteins.

On the other hand, NMR spectra show no major structural differences. Signal dispersion remained very poor, preventing any detailed study of the interaction (Figure 4). Nevertheless, some new features can be observed upon incubation of both proteins. The Trp40 signal from P1α shifts from its original position in the protein alone to lower field values. Some new signals also arise in the aliphatic region, which could be indicative of a higher degree of structure. Therefore, P1α Trp40 seems to be involved in the interaction between both proteins. Furthermore, P1α Trp40 fluorescence emission is enhanced when P2*β* is present (Figure 9B). Even though fluorescence quenching and protein aggregation prevented a detailed study of the interaction at high protein concentrations, an estimated value of $0.5-0.6\cdot10^{-6}$ M was obtained for the binding constant of the P1α/P2*β* interaction.

It is important to take note of the fact that the affinity of both P1α and P2*β* to form self-oligomers is lower than that observed for the formation of P1α-P2*β* hetero-complexes, since the latter are formed at concentrations as low as nanomolar, whereas the former appear at clearly higher concentrations. Even P2*β*, which is more prone to aggregation, forms homo-dimers only at micromolar concentrations (*36*), clearly indicating that its affinity to bind P1α is higher than its affinity to bind itself.

DISCUSSION

This study clearly shows that the yeast ribosomal acidic P1α protein is not a compact polypeptide when in solution and is detected as a rather unfolded protein by different experimental approaches. Similar conclusions were previously obtained in the case of another yeast stalk component, protein P2*β* (*36*). The accumulation of experimental data describing unstructured proteins is confirming their importance in many physiological processes as has been recently reviewed (*59*). The stalk proteins seem to be a relevant case of unfolded polypeptides. Flexibility seems to be an important requirement for the function of the ribosomal P proteins and enables them to interact with diverse different ribosomal regions (*60*, *61*). In fact, the mobility of these stalk components in prokaryotic as well as in eukaryotic ribosomes has been experimentally confirmed by NMR (*62*).

Interestingly, the α-helical content predictions for both P1α and P2*β* are higher than the experimentally estimated values. This could be due to the absence of tertiary and/or long-range contacts, which are reported to stabilize and increase the secondary structure content in proteins (*63*, *64*). It is quite possible that the secondary structure of the proteins could be stabilized by the formation of nonlocal interactions upon binding to the ribosome or through interactions with other proteins (see below). The similarity in the predicted secondary structure content for both proteins stresses their similarity in sequence and suggests that their final conformation, once bound to the ribosome, could be similar.

Different Functions and Different Structural Features. Previous experimental data indicated that, despite their close amino acid sequence similarity, the two stalk protein types play different roles in the ribosome function (*31*, *33*). These functional differences have been confirmed using an in vitro stalk reconstitution approach (*34*). The results in this report show that the different functional role could be related to structural differences between both proteins. Even though neither protein is folded in solution under physiological pH and temperature conditions, P1α shows a lower secondary structure content than P2*β*. Nevertheless, the high sequence homology between both proteins and the similarity in secondary structure predictions seem to point to some local amino acid changes as being responsible for the observed differences. It is important to note that P1α shows a higher concentration of acidic residues in the N-terminal region of the protein than its counterpart, P2*β* (see Figure 1). The fact that P1α increases its secondary structure content when the pH is lowered, whereas P2*β* remains unaltered under similar conditions (*36*), suggests that secondary structure destabilization by local charge repulsion of one or several acidic residues might take place in P1α at a neutral pH. Thus, these residues would become protonated when the pH is decreased, and their repulsive effect would be canceled, favoring the stabilization the secondary structure in that region. Analysis of the secondary structure propensities of P1α by AGADIR (*65*, *66*) indicates that the substitution of a single acidic residue (Asp16) by asparagine (emulating protonation at low pH) enhances the local helical propensity of the protein. This propensity is enhanced even more when substitution of Asp16 by Ala is introduced (data not shown). Even though these predictions have to be studied in more detail, they provide a good explanation for the changes in secondary structure content experienced by P1α at different pH values and also for the differences in secondary structure content between such a closely related pair of proteins P1α and P2*β*.

Some important differences in the thermal denaturation profiles of both proteins also show up at physiological pH. P2*β* shows a low cooperative thermal denaturation profile when temperature is increased (*36*). On the contrary, P1α displays a loss of secondary structure at temperatures below 30 °C. These findings are compatible with the existence of some residual secondary structure in P1α at physiological temperatures, albeit it must be quite reduced in comparison with that one exhibited by P2*β*. Nevertheless, since this residual structure is present at near physiological, it could be important for the functional role of P1α.

The fact that P1α shows lower structuration than its P2*β* counterpart may also be directly related to the physiological regulation of both proteins. Thus, as commented on previously, while the P2 proteins can accumulate free in the yeast cytoplasm, the P1 proteins are quickly degraded under the same conditions, although they are protected by the presence of P2 polypeptides (G. Nusspaumer, M. Remacha, and J. P. G. Ballesta, unpublished results). The high resistance to degradation of P2*β* in the cell is, nonetheless, quite unexpected considering its low structuration and its in vitro sensitivity to proteinase K in the absence of TFE. Therefore, the association of these proteins with other shielding polypeptides that can affect their regulation as well as their assembly into the ribosomal stalk is quite possible.

Protein−Protein Interaction and Possible Physiological Implications. The available biochemical and genetic data indicate that there must be an interaction between P1α and

P2β in the ribosome as well as in the cytoplasm. This interaction is supported here by the gain in secondary structure observed upon mixing both proteins, probably due to stabilization of helical-prone regions. Moreover, NMR data show a shift of the P1α Trp40 signal under similar conditions, suggesting that this part of the protein is directly involved in the interaction between both proteins. Such an interaction seems, in any case, to be associated with a local increase in α-helix in one or both of the proteins, albeit no major tertiary reorganization or compaction was observed, as this would notably alter the signal dispersion in the NMR spectrum.

Furthermore, the partial gain in structure experienced by the complex could supply enough elements to facilitate the activity of the P1α protein once bound to the ribosome. In this way, whereas P1α provides a link for the binding of P2β to the ribosome, P2β could increase P1α functionality by inducing new structural features after their interaction. In addition, the structural changes observed after the interaction of P1α with P2β could increase P1α resistance to proteolysis. This could provide an explanation for the higher stability observed for P1α in vivo when P2 proteins are also present in the cell (G. Nusspaumer, M. Remacha, and J. P. G. Ballesta, unpublished results; ref *34*).

The available data indicate that the prokaryotic L7/L12 and the eukaryotic P proteins exhibit very different topologies (*67*). As reported previously, only the "hinge" region shows some degree of homology between both families of proteins, but its location in the sequence is quite different (*36*). The N-terminus domain in eukaryotic P proteins is larger than in bacterial L12, whereas the C-terminus domain is restricted in the former to a small peptide (12−15 residues long) with very little structure in solution (J. Zurdo, C. González, M. Rico, and J. P. G. Ballesta, unpublished results). Consequently, the P proteins have no "core", or compact carboxyl domain, as opposed to their prokaryotic counterparts (*35*, *36*, *68*).

Nevertheless, data from prokaryotic systems can provide valuable elements to understand the behavior of their eukaryotic counterparts. In this way, a structural characterization of the prokaryotic protein L12 by X-ray diffraction has recently shown the acquisition of a helical structure in the hinge region upon dimerization (*69*). A similar process could explain the increase in secondary structure that has been reported upon P1α−P2β interaction. In fact, the formation of P1α−P2β hetero-complexes, which takes place at nanomolar concentration, involves an increase in the helical secondary structure content of the proteins. Therefore, a process similar to the one reported by Wahl and co-workers for protein L12 (*69*) could possibly occur upon P1α−P2β association in solution. Moreover, our results point to a preribosomal P1α−P2β interaction as a possible mechanism for P2β binding to the ribosome and provide a regulatory element which would account for some physiological data.

In contrast, the divergence in helical structure content between P1α and P2β proteins does not seem to be based on their different self-association propensities. This can be clearly proven for P2β. The CD spectral features of this protein are invariable although self-association occurs and an equilibrium exists among different species, which fluctuates with the global protein concentration (*36*). Accordingly, the same secondary structure content appears either when the protein is mainly monomeric or when dimers and tetramers accumulate in solution.

Taken together, these findings support the idea that different ribosomal acidic proteins can be connected to specific ribosomal activities through subtle structural differences and interactions between them. In this sense, phosphorylation, which is a typical feature of these proteins in the cell, would increase the number of possible options. In fact, it has been shown that this modification, although it does not affect the interaction of the proteins with the ribosome, can somehow modulate the activity of the ribosomal stalk (*38*, *70*, *71*).

The fact that eukaryotic cells have two different ribosomal acidic families (P1 and P2) while prokaryotic ones have only one, seems to suggest a specialization or distribution of functions between both families, giving rise to a higher complexity of regulation and, therefore, of action. This concept seems to be supported by the data showing how two very similar proteins can have a significantly different behavior. Thus, it is possible that by "tuning" proteins through minor modifications in sequence, a high range of functional choices will appear. The question that still remains open is to find out why some eukaryotes, like yeast, protozoa, and plants, have several ribosomal acidic proteins of the same type, whereas mammals can cope with only two. Perhaps higher requirements for "metabolic" adaptability may be in the origin of such expansion.

ACKNOWLEDGMENT

We thank M.C. Fernandez Moyano for expert technical assistance and Dr. Germán Bou for help with the construction of the P1α expression vector.

REFERENCES

1. Agalarov, S. C., Zheleznyakova, E. N., Selivanova, O. M., Zheleznaya, L. A., Matvienko, N. I., Vasiliev, V. D., and Spirin, A. S. (1998) *Proc. Natl. Acad. Sci. U.S.A. 95*, 999−1003.
2. Strycharz, W. A., Nomura, M., and Lake, J. A. (1978) *J. Mol. Biol. 126*, 123−140.
3. Marquis, D. M., Fahnestock, S. R., Henderson, E., Woo, D., Schwinge, D., Clark, M., and Lake, J. A. (1981) *J. Mol. Biol. 150*, 121−132.
4. Pettersson, I., Hardy, S. J., and Liljas, A. (1976) *FEBS Lett. 64*, 135−138.
5. Gudkov, A. T., Tumanova, L. G., Vanyaminov, Y. S., and Khechinashvilli, N. M. (1978) *FEBS Lett. 93*, 215−218.
6. Dijk, J., Garrett, R. A., and Müller, R. (1979) *Nucleic Acids Res. 6*, 2717−2729.
7. Beauclerk, A. D., Cundliffe, E., and Dijk, J. (1984) *J. Biol. Chem. 259*, 6559−6563.
8. Möller, W., and Maassen, J. A. (1986) in *Structure, function and genetics of ribosomes* (Hardesty, B., and Kramer, G., Eds.) pp 309−325, Springer-Verlag, New York.
9. Stark, H., Rodnina, M. V., Rinke-Appel, J., Brimacombe, R., Wintermeyer, W., and van Heel, M. (1997) *Nature 389*, 403−406.
10. Agrawal, R. K., Penzek, P., Grassucci, R. A., and Frank, J. (1998) *Proc. Natl. Acad. Sci. U.S.A. 95*, 6134−6138.
11. Lake, J. W., Henderson, E., Oakes, M., and Clark, M. W. (1984) *Proc. Natl. Acad. Sci. U.S.A. 81*, 3786−3790.
12. Ballesta, J. P. G., and Remacha, M. (1996) *Prog. Nucl. Acids Res. Mol. Biol. 55*, 157−193.
13. Matheson, A. T., Louie, K. A., and Henderson, G. N. (1986) *Syst. Appl. Microbiol. 7*, 147−150.
14. Casiano, C., Matheson, A. T., and Traut, R. R. (1990) *J. Biol. Chem. 265*, 18757−18761.

15. Mache, R., Stutz, E., and Subramanian, A. R. (1991) *NATO ASI Series*, Springer-Verlag, Heidelberg.
16. Sanchez-Madrid, F., Reyes, R., Conde, P., and Ballesta, J. P. G. (1979) *Eur. J. Biochem. 98*, 409−416.
17. MacConnell, W. P., and Kaplan, N. O. (1980) *Biochem. Biophys. Res. Commun. 92*, 46−52.
18. Köpke, A. K. E., Leggatt, P. A., and Matheson, A. T. (1992) *J. Biol. Chem. 267*, 1382−1390.
19. Wool, I. G., Chan, Y. L., Glück, A., and Suzuki, K. (1991) *Biochimie 73*, 861−870.
20. Zinker, S., and Warner, J. R. (1976) *J. Biol. Chem. 251*, 1799−1807.
21. van Agthoven, A. J., Maassen, J. A., and Möller, W. (1977) *Biochem. Biophys. Res. Commun. 77*, 989−998.
22. Kruiswijk, T., de Hey, J. T., and Planta, R. J. (1978) *Biochem. J. 175*, 213-219.
23. Lin, A., Wittman-Leibold, B., McNelly, T., and Wool, I. G. (1982) *J. Biol. Chem. 257*, 9189−9197.
24. Szick, K., Springer, M., and Bailey-Serres, J. (1998) *Proc. Natl. Acad. Sci. U.S.A. 95*, 2378−2383.
25. Mager, W. H., Planta, R. J., Ballesta, J. G., Lee, J. C., Mizuta, K., Suzuki, K., Warner, J. R., and Woolford, J. (1997) *Nucleic Acid Res. 25*, 4872−4875.
26. Uchiumi, T., and Kominami, R. (1992) *J. Biol. Chem. 267*, 19179−19185.
27. Tsurugi, K., and Ogata, K. (1985) *J. Biochem. 98*, 1427−1431.
28. Scharf, K.-D., and Nover, L. (1987) *Biochim. Biophys. Acta 909*, 44−57.
29. Towbin, G., Siegmann, M., and Gordon, J. (1982) *J. Biol. Chem. 257*, 12709−12715.
30. Isono, S., and Isono, K. (1981) *Mol. Gen. Genet. 183*, 473−477.
31. Remacha, M., Santos, C., and Ballesta, J. P. G. (1990) *Mol. Cell. Biol. 10*, 2182−2190.
32. Payo, J. M., Santana-Roman, H., Remacha, M., Ballesta, J. P. G., and Zinker, S. (1995) *Biochemistry 34*, 7941−7948.
33. Remacha, M., Santos, C., Bermejo, B., Naranda, T., and Ballesta, J. P. G. (1992) *J. Biol. Chem. 267*, 12061−12067.
34. Zurdo, J., van den Berg, A., Parada, P., Nusspaumer, G., Jimenez-Diaz, A., Remacha, M., and Ballesta, J. P. G. (2000) *Biochemistry 39*, 8929−8934.
35. Leijonmarck, M., Eriksson, S., and Liljas, A. (1980) *Nature 286*, 824−826.
36. Zurdo, J., Sanz, J. M., Gonzalez, C., Rico, M., and Ballesta, J. P. G. (1997) *Biochemistry 36*, 9625−9635.
37. Studier, F. W., Rosenberg, A. H., Dunn, J. J., and Dubendorff, J. W. (1990) *Methods Enzymol. 185*, 60−89.
38. Zambrano, R., Briones, E., Remacha, M., and Ballesta, J. P. G. (1997) *Biochemistry 36*, 14439−14446.
39. Vilella, M. D., Remacha, M., Ortiz, B. L., Mendez, E., and Ballesta, J. P. G. (1991) *Eur. J. Biochem. 196*, 407−414.
40. Newton, C. H., Shimmin, L. C., Yee, J., and Dennis, P. P. (1990) *J. Bacteriol. 172*, 579−588.
41. Santos, C., Ortiz-Reyes, B. L., Naranda, T., Remacha, M., and Ballesta, J. P. G. (1993) *Biochemistry 32*, 4231−4236.
42. Gill, S. C., and von Hippel, P. V. (1989) *Anal. Biochem. 182*, 319−326.
43. Rost, B., and Sander, C. (1993) *J. Mol. Biol. 232*, 584−599.
44. Rost, B., and Sander, C. (1993) *Proc. Natl. Acad. Sci. U.S.A. 90*, 7558−7562.
45. Rost, B., and Sander, C. (1994) *Proteins 19*, 55−72.
46. Bohm, G., Muhr, R., and Jaenicke, R. (1992) *Protein Eng. 5*, 191−195.
47. Andrade, M. A., Chacon, P., Merelo, J. J., and Moran, F. (1993) *Protein Eng. 6*, 383−90.
48. Deleage, G., and Geourjon, C. (1993) *Comput. Appl. Biosci. 9*, 197−199.
49. Bolotina, I. A., Chekhov, V. O., Lugauskas, V., and Ptitsyn, O. B. (1980) *Mol. Biol. (USSR) 14*, 902−909.
50. Chen, Y.-H., Yang, J. T., and Chau, K. H. (1974) *Biochemistry 13*, 3350−3359.
51. Sreerama, N., and Woody, R. W. (1994) *Biochemistry 33*, 10022−10025.
52. Compton, L. A., and Johnson, W. C., Jr. (1986) *Anal. Biochem. 155*, 155−167.
53. Manavalan, P., and Johnson, W. C., Jr. (1987) *Anal. Biochem. 167*, 76−85.
54. Eftink, M. R., and Ghiron, C. A. (1981) *Anal. Biochem. 114*, 199−227.
55. Lehrer, S. S. (1971) *Biochemistry 10*, 3254−3263.
56. Dahlquist, F. W. (1978) *Methods Enzymol. 48*, 270−299.
57. Schaegger, H., and von Jagow, G. (1987) *Anal. Biochem. 166*, 368−379.
58. Rodger, A., and Nordén, B. (1997) *Circular cichroism and linear dichroism*, Oxford University Press, New York.
59. Wright, P. E., and Dyson, H. J. (1999) *J. Mol. Biol. 293*, 321−331.
60. Zecherle, G. N., Oleinikov, A., and Traut, R. R. (1992) *J. Biol. Chem. 267*, 5889−5896.
61. Dey, D., Bochkariov, D. E., Jokhadze, G. G., and Traut, R. R. (1998) *J. Biol. Chem. 273*, 1670−1676.
62. Cowgill, C. A., Nichols, B. G., Kenny, J. W., butler, P., Bradbury, E. M., and Traut, R. R. (1984) *J. Biol. Chem. 259*, 15257−15263.
63. Woody, R. W. (1994) in *Circular dichroism principles and applications* (Nakanishi, K., Berova, N., and Woody, R. W., Eds.) VCH, New York.
64. Johnson, W. C., Jr. (1990) *Proteins 7*, 205−214.
65. Munoz, V., and Serrano, L. (1995) *Curr. Opin. Biotechnol. 6*, 382−386.
66. Munoz, V., and Serrano, L. (1997) *Biopolymers 41*, 495−509.
67. Shimmin, L. C., Ramirez, G., Matheson, A. T., and Dennis, P. P. (1989) *J. Mol. Evol. 29*, 448−462.
68. Todorova, R. T., Rogov, V. V., Vasilenko, K. S., and Permyakov, E. A. (1996) *Biophys. Chem. 62*, 39−45.
69. Wahl, M. C., Bourenkov, G. P., Bartunik, H. D., and Huber, R. (2000) *Embo. J. 19*, 174−86.
70. Rodriguez-Gabriel, M. A., Remacha, M., and Ballesta, J. P. G. (1998) *Biochemistry 37*, 16620−16626.
71. Bargis-Surgey, P., Lavergne, J. P., Gonzalo, P., Vard, C., Filhol-Cochet, O., and Reboud, J. P. (1999) *Eur. J. Biochem. 262*, 606−611.

BI000363B